

# A new locking-free brick element formulation for continuous large deformation problems

S. Reese\*, P. Wriggers\* & B. D. Reddy°

\*Darmstadt University of Technology  
Institute of Mechanics  
Hochschulstr. 1, D-64289 Darmstadt, Germany

°University of Cape Town  
FRD/UCT Centre for Research  
in Computational and Applied Mechanics  
7700 Rondebosch, South Africa

April 1, 1998

**Key Words:** hourglass stabilization, reduced integration, enhanced strain method, shell, incompressibility, stability

## Abstract

In the present contribution, an innovative brick element formulation for large deformation problems in finite elasticity is discussed. The new formulation can be considered as a reduced integration plus stabilization concept with the stabilization factors being computed on the basis of the enhanced strain method. Such an idea has not been applied yet in the context of large deformation 3D problems and leads to a surprisingly well-behaved locking-free element formulation. Crucial to the method is the notion of the so-called equivalent parallelepiped. The major advantages of the new formulation are its simplicity and robustness. Since the element quantities are evaluated only in the center of the element, the approach is also very efficient from the numerical point of view.

## 1 Introduction

Isoparametric low-order elements are very popular due to their robustness and simplicity. Moreover, the application of such elements leads to an advantageous band structure which is particularly important for systems with many degrees of freedom. A major disadvantage, however, is the so-called locking effect which arises mainly in bending-dominated situations and in the limit of incompressibility. In order to overcome this difficulty in large deformation problems, mainly multi-field methods have been developed which either work only against the volumetric locking (see the “B-Bar method” of Simo et al.<sup>1</sup> or eliminate the effect completely (Simo and Armero<sup>2</sup>, Simo et al.<sup>3</sup>). It has become evident quite recently, that element formulations of the latter type react very sensitively in many applications. Numerical (non-physical) instabilities are observed for such simple examples as a block under homogeneous compression (Wriggers and Reese<sup>4</sup>, De Souza Neto et al.<sup>5</sup>). There have been several attempts to overcome the problem (see e. g. Crisfield et al.<sup>6</sup>, Korelc and Wriggers<sup>7</sup>, Glaser and Armero<sup>8</sup> and Kasper and Taylor<sup>9</sup> to name only a few). But an explanation for the hourglass instability effect is still missing. Thus, one can never be sure that the effect does not arise in a situation which has not been tested before. Moreover, many new formulations are rather elaborate and difficult to code. Another major drawback is the computational inefficiency which is caused by numerous matrix operations on element level, and the necessity to store a large number of history variables. Finally, higher order quadrature rules are sometimes necessary to obtain stable behaviour.

Therefore, the goal of the present work is primarily to develop a very simple and efficient element formulation which shows robust and stable deformation behaviour in the classically difficult examples, like e. g. thin shell problems and compression tests. The results are comparable with those of the enhanced strain method or the B-Bar method. The suggested formulation is very similar to the classical stabilization concept originally developed by Belytschko and coworkers (see e. g. Flanagan and Belytschko<sup>10</sup>, Belytschko et al.<sup>11</sup> and Belytschko and Bachrach<sup>12</sup> for the geometrically linear theory). The main difficulty of the method lies in the computation of the stabilization factors. For this purpose, Belytschko and coworkers exploited the important papers of Kosloff and Frazier<sup>13</sup> and Malkus and Hughes<sup>14</sup> who were able to show the connection between the stabilization concept and a mixed formulation based on the Hu-Wahizu principle. In the context of large deformations, however, this idea is new and has been employed up to now only in the work of Reese et al.<sup>15</sup> for plane strain problems. Crucial to this new formulation is the concept of the equivalent parallelogram which has been introduced and further investigated by Arunakirinathar and Reddy<sup>16,17</sup>. The notion of an equivalent parallelepiped can be analogously developed (Küssner and Reddy<sup>18</sup>), although its construction is certainly more complicated.

One of the important points of the present paper is the observation that the calculation of the stabilization factors can be based either on the material tangent or on the full tangent. Using only the material tangent provides excel-

lent performance in compression tests, whereas the full tangent has to be taken into account in order to obtain a locking-free response in bending-dominated problems. Note that the enhanced strain approach is naturally always based on the full tangent. This might explain why the problem of hourglass instabilities arises particularly in compression.

In order to extend the approach to three dimensions, we follow only partially the line of the previous paper. This is due to the appearance of tri-linear terms in the shape functions which lead to volumetric locking and require a special treatment (see Simo et al.<sup>3</sup>, Korelc and Wriggers<sup>19</sup>). Another new aspect concerns the dependence of the results on the size of the load step. Usually, the influence is of minor importance, but the undesirable purely numerical effect can be eliminated by a simple after-iteration procedure. The latter point is crucial to the modeling of thin shell applications.

## 2 Variational formulation

We start from the standard weak formulation in finite elasticity

$$g = \hat{g}(\mathbf{u}, \mathbf{v}) = \int_{\mathcal{B}_0} \frac{\partial \hat{W}(\text{Grad } \mathbf{u})}{\partial \text{Grad } \mathbf{u}} : \text{Grad } \mathbf{v} \, dV - \hat{g}_a(\mathbf{v}) = 0 \quad (1)$$

which is derived from the balance of linear momentum

$$\text{Div} \frac{\partial \hat{W}(\text{Grad } \mathbf{u})}{\partial \text{Grad } \mathbf{u}} + \mathbf{f} = \mathbf{0}. \quad (2)$$

In (1), the short hand notation

$$g_a = \hat{g}_a(\mathbf{v}) = \int_{\mathcal{B}_0} \mathbf{f} \cdot \mathbf{v} \, dV + \int_{\mathcal{B}_P} \bar{\mathbf{t}} \cdot \mathbf{v} \, dA \quad (3)$$

has been introduced for the terms related to the external loading. In order to develop (1), we exploit the constitutive law  $\mathbf{P} = \frac{\partial W}{\partial \mathbf{H}}$  and the kinematic relation  $\mathbf{H} = \text{Grad } \mathbf{u}$ , where  $\mathbf{P}$  denotes the first Piola-Kirchhoff stress tensor,  $\mathbf{f}$  describes the vector of body forces and  $\mathbf{H}$  represents a so-called physical strain tensor which is set equal to the displacement gradient  $\text{Grad } \mathbf{u}$ . Hyperelastic material behaviour is assumed, such that the first Piola-Kirchhoff stress tensor can be derived from a potential, the strain energy per reference volume  $W = \hat{W}(\mathbf{H})$ . The function  $\hat{W}(\mathbf{H})$  is chosen in such a way that the material law is invariant with respect to rigid body motions. Furthermore, we prescribe tractions  $\mathbf{t} = \mathbf{P} \cdot \mathbf{n} = \bar{\mathbf{t}}$  on the boundary  $\partial \mathcal{B}_P$  and displacements  $\mathbf{u} = \bar{\mathbf{u}}$  on  $\partial \mathcal{B}_u$ . Only dead loading is considered. Note that  $\partial \mathcal{B}_0 = \partial \mathcal{B}_P \cup \partial \mathcal{B}_u$  and  $\partial \mathcal{B}_P \cap \partial \mathcal{B}_u = \emptyset$ . The vector  $\mathbf{n}$  represents the outward unit vector normal to  $\partial \mathcal{B}_0$ . The vector-valued test function  $\mathbf{v}$  is defined on the space of displacements

$$\mathcal{V} = \{\mathbf{v} \mid v_i \in H^1(\mathcal{B}_0), \mathbf{v} = \mathbf{0} \text{ on } \partial \mathcal{B}_u\}. \quad (4)$$

In the discrete case, the weak form is defined on the finite-dimensional subspace  $\mathcal{V}^h \subset \mathcal{V}$ . The discrete variational problem then reads

$$\hat{g}(\mathbf{u}^h, \mathbf{v}^h) = \int_{\mathcal{B}_0^h} \frac{\partial \hat{W}^h(\text{Grad } \mathbf{u}^h)}{\partial \text{Grad } \mathbf{u}^h} : \text{Grad } \mathbf{v}^h dV^h - \hat{g}_a(\mathbf{v}^h) = 0. \quad (5)$$

### 3 Finite element formulation

#### 3.1 Hourglass stabilization in the small deformation case

In order to make the present approach more transparent, we start with the review of the stabilization procedure in the context of small deformations. The method is based on the isoparametric trilinear standard interpolation which can be written for  $\mathbf{u}^h = u_i^h \mathbf{e}_i$  in the form

$$u_1^h = \mathbf{N}^T \mathbf{d}_1; \quad u_2^h = \mathbf{N}^T \mathbf{d}_2; \quad u_3^h = \mathbf{N}^T \mathbf{d}_3. \quad (6)$$

In these equations,  $\mathbf{N}$  is formulated by means of

$$\begin{aligned} \mathbf{N} &= \frac{1}{8} \begin{Bmatrix} 1 \\ 1 \\ 1 \\ 1 \\ 1 \\ 1 \\ 1 \\ 1 \end{Bmatrix} + \xi \frac{1}{8} \begin{Bmatrix} 1 \\ -1 \\ -1 \\ 1 \\ 1 \\ -1 \\ -1 \\ 1 \end{Bmatrix} + \eta \frac{1}{8} \begin{Bmatrix} -1 \\ -1 \\ 1 \\ 1 \\ -1 \\ -1 \\ 1 \\ 1 \end{Bmatrix} + \zeta \frac{1}{8} \begin{Bmatrix} -1 \\ -1 \\ -1 \\ -1 \\ 1 \\ 1 \\ 1 \\ 1 \end{Bmatrix} \\ &+ \xi \eta \frac{1}{8} \begin{Bmatrix} 1 \\ -1 \\ 1 \\ -1 \\ 1 \\ -1 \\ 1 \\ -1 \end{Bmatrix} + \eta \zeta \frac{1}{8} \begin{Bmatrix} 1 \\ 1 \\ -1 \\ -1 \\ -1 \\ 1 \\ 1 \\ 1 \end{Bmatrix} + \zeta \xi \frac{1}{8} \begin{Bmatrix} 1 \\ -1 \\ -1 \\ 1 \\ 1 \\ -1 \\ -1 \\ 1 \end{Bmatrix} + \xi \eta \zeta \frac{1}{8} \begin{Bmatrix} -1 \\ 1 \\ -1 \\ 1 \\ 1 \\ -1 \\ 1 \\ -1 \end{Bmatrix} \\ &= \mathbf{r} + \xi \mathbf{g}_\xi + \eta \mathbf{g}_\eta + \zeta \mathbf{g}_\zeta + \xi \eta \mathbf{h}_{\xi\eta} + \eta \zeta \mathbf{h}_{\eta\zeta} + \zeta \xi \mathbf{h}_{\zeta\xi} + \xi \eta \zeta \mathbf{h}_{\xi\eta\zeta} \end{aligned} \quad (7)$$

and the vectors  $\mathbf{d}_i$  ( $i = 1, 2, 3$ ) contain the nodal displacements in  $i$ -direction. Note that from now on we use matrix notation, with matrices being denoted by boldface italic letters. The coordinates  $\xi, \eta, \zeta$  are local coordinates defined on the reference domain  $\Omega_e = [-1, 1] \times [-1, 1] \times [-1, 1]$ .

The weak form (5) reduces in the case of small deformations to

$$\hat{g}^l(\mathbf{u}^h, \delta \mathbf{u}^h) = \int_{\mathcal{B}_0^h} (\delta \boldsymbol{\varepsilon}^h)^T \mathcal{C}_0 \boldsymbol{\varepsilon}^h dV^h - \hat{g}_a(\delta \mathbf{u}^h) = 0, \quad (8)$$

where the linearized strain vector  $\boldsymbol{\varepsilon}^h$  and the material matrix of linear elasticity  $\mathcal{C}_0$  have been introduced. Further,  $\mathbf{v}^h$  is assumed to be identical with the variation  $\delta\mathbf{u}^h$ . The weak form upon which the enhanced strain method is based can be easily derived by splitting the strain vector  $\boldsymbol{\varepsilon}^h$  in a compatible part  $\boldsymbol{\varepsilon}_{\text{comp}}^h$  and a so-called enhanced (or incompatible) part  $\boldsymbol{\varepsilon}_{\text{enh}}^h$ . See for more details e. g. Simo and Rifai<sup>20</sup>. The variational formulation (8) then takes the form

$$\begin{aligned} g_{\text{enh}}^l &= \hat{g}_{\text{enh}}^l(\mathbf{u}^h, \delta\mathbf{u}^h, \boldsymbol{\varepsilon}_{\text{enh}}^h, \delta\boldsymbol{\varepsilon}_{\text{enh}}^h) \\ &= \int_{\mathcal{B}_0^h} (\delta\boldsymbol{\varepsilon}_{\text{comp}}^h + \delta\boldsymbol{\varepsilon}_{\text{enh}}^h)^T \mathcal{C}_0 (\boldsymbol{\varepsilon}_{\text{comp}}^h + \boldsymbol{\varepsilon}_{\text{enh}}^h) dV^h - \hat{g}_a(\delta\mathbf{u}^h) = 0. \end{aligned} \quad (9)$$

Using the interpolation (7) for the compatible strains and approximating the incompatible strain vector by means of the ‘‘bubble’’ functions of Wilson et al.<sup>21</sup> yields

$$\boldsymbol{\varepsilon}_{\text{comp}}^h = \underbrace{\begin{bmatrix} \frac{\partial}{\partial X_1} & 0 & 0 \\ 0 & \frac{\partial}{\partial X_2} & 0 \\ 0 & 0 & \frac{\partial}{\partial X_3} \\ \frac{\partial}{\partial X_2} & \frac{\partial}{\partial X_1} & 0 \\ 0 & \frac{\partial}{\partial X_3} & \frac{\partial}{\partial X_2} \\ \frac{\partial}{\partial X_3} & 0 & \frac{\partial}{\partial X_1} \end{bmatrix}}_{\mathbf{B}} \begin{bmatrix} \mathbf{N}^T & \mathbf{0}^T & \mathbf{0}^T \\ \mathbf{0}^T & \mathbf{N}^T & \mathbf{0}^T \\ \mathbf{0}^T & \mathbf{0}^T & \mathbf{N}^T \end{bmatrix} \begin{Bmatrix} \mathbf{d}_1 \\ \mathbf{d}_2 \\ \mathbf{d}_3 \end{Bmatrix} \quad (10)$$

$$\boldsymbol{\varepsilon}_{\text{enh}}^h = \underbrace{\begin{bmatrix} \frac{\partial}{\partial X_1} & 0 & 0 \\ 0 & \frac{\partial}{\partial X_2} & 0 \\ 0 & 0 & \frac{\partial}{\partial X_3} \\ \frac{\partial}{\partial X_2} & \frac{\partial}{\partial X_1} & 0 \\ 0 & \frac{\partial}{\partial X_3} & \frac{\partial}{\partial X_2} \\ \frac{\partial}{\partial X_3} & 0 & \frac{\partial}{\partial X_1} \end{bmatrix}}_{\mathbf{G}} \begin{bmatrix} \mathbf{P}^T & \mathbf{0}^T & \mathbf{0}^T \\ \mathbf{0}^T & \mathbf{P}^T & \mathbf{0}^T \\ \mathbf{0}^T & \mathbf{0}^T & \mathbf{P}^T \end{bmatrix} \begin{Bmatrix} \mathbf{p}_1 \\ \mathbf{p}_2 \\ \mathbf{p}_3 \end{Bmatrix} \quad (11)$$

where  $\mathbf{P}^T = \{\frac{1}{2}(1-\xi^2), \frac{1}{2}(1-\eta^2), \frac{1}{2}(1-\zeta^2)\}$  and the coefficients of each vector  $\mathbf{p}_i$  ( $i = 1, 2, 3$ ) represent three internal degrees of freedom.

The next step is to carry out a Taylor expansion of  $\mathbf{N}$  around the center of the element  $\boldsymbol{\xi} = \mathbf{0}$ . This leads after some analysis to

$$\begin{aligned} \mathbf{N} &= \mathbf{N}_0 + \left. \frac{\partial \mathbf{N}}{\partial \mathbf{X}} \right|_{\boldsymbol{\xi}=\mathbf{0}} (\mathbf{X} - \mathbf{X}_0) + \mathbf{N}_{\text{hg}} \\ &= \mathbf{N}_0 + \left. \frac{\partial \mathbf{N}}{\partial \boldsymbol{\xi}} \right|_{\boldsymbol{\xi}=\mathbf{0}} \mathbf{J}_0^{-1} (\mathbf{X} - \mathbf{X}_0) + \mathbf{N}_{\text{hg}} \\ &= \underbrace{\mathbf{N}_0 + [\mathbf{b}_1 \quad \mathbf{b}_2 \quad \mathbf{b}_3]}_{\mathbf{N}_{\text{lin}}} (\mathbf{X} - \mathbf{X}_0) + \mathbf{N}_{\text{hg}}. \end{aligned} \quad (12)$$

The ‘‘hourglass’’ part of  $\mathbf{N}$  takes the form

$$\begin{aligned} \mathbf{N}_{\text{hg}} &= \left( \mathbf{1}^8 - [ \mathbf{b}_1 \quad \mathbf{b}_2 \quad \mathbf{b}_3 ] \mathbf{X}^{\text{node}} \right) \\ &\quad \left( \xi \eta \mathbf{h}_{\xi\eta} + \eta \zeta \mathbf{h}_{\eta\zeta} + \zeta \xi \mathbf{h}_{\zeta\xi} + \xi \eta \zeta \mathbf{h}_{\xi\eta\zeta} \right) \\ &= \xi \eta \boldsymbol{\gamma}_{\xi\eta} + \eta \zeta \boldsymbol{\gamma}_{\eta\zeta} + \zeta \xi \boldsymbol{\gamma}_{\zeta\xi} + \xi \eta \zeta \boldsymbol{\gamma}_{\xi\eta\zeta}, \end{aligned} \quad (13)$$

where the so-called stabilization vectors  $\boldsymbol{\gamma}_{\xi\eta}$ ,  $\boldsymbol{\gamma}_{\eta\zeta}$ ,  $\boldsymbol{\gamma}_{\zeta\xi}$ ,  $\boldsymbol{\gamma}_{\xi\eta\zeta}$  are introduced. In the latter equation, the matrix  $\mathbf{X}^{\text{node}}$  is a  $3 \times 8$  matrix containing the coordinates of the element nodes. The vector  $\mathbf{X}$  is described by  $\mathbf{X}^T = \{X_1, X_2, X_3\}$  and  $\mathbf{X}_0$  contains the cartesian coordinates of the center of the element.  $\mathbf{J}_0$  denotes the Jacobian matrix  $\mathbf{J} = \frac{\partial \mathbf{X}}{\partial \boldsymbol{\xi}}$  evaluated at  $\boldsymbol{\xi} = \{\xi, \eta, \zeta\} = \mathbf{0}$ . See for more details the original derivation in the paper of Belytschko et al.<sup>11</sup> [1984]. In order to make the following analysis more transparent, we exploit the representation of Hansbo<sup>22</sup> and write the matrix  $\mathbf{B}$  as

$$\mathbf{B} = \mathbf{j} (\hat{\mathbf{B}}_{\text{lin}} \mathbf{M}_{\text{lin}} + \hat{\mathbf{B}}_{\text{hg}} \mathbf{M}_{\text{hg}}), \quad (14)$$

where

$$\mathbf{j} = \begin{bmatrix} \frac{\partial \xi}{\partial X_1} & \frac{\partial \eta}{\partial X_1} & \frac{\partial \zeta}{\partial X_1} & 0 & 0 & 0 & 0 & 0 & 0 \\ 0 & 0 & 0 & \frac{\partial \xi}{\partial X_2} & \frac{\partial \eta}{\partial X_2} & \frac{\partial \zeta}{\partial X_2} & 0 & 0 & 0 \\ 0 & 0 & 0 & 0 & 0 & 0 & \frac{\partial \xi}{\partial X_3} & \frac{\partial \eta}{\partial X_3} & \frac{\partial \zeta}{\partial X_3} \\ \frac{\partial \xi}{\partial X_2} & \frac{\partial \eta}{\partial X_2} & \frac{\partial \zeta}{\partial X_2} & \frac{\partial \xi}{\partial X_1} & \frac{\partial \eta}{\partial X_1} & \frac{\partial \zeta}{\partial X_1} & 0 & 0 & 0 \\ 0 & 0 & 0 & \frac{\partial \xi}{\partial X_3} & \frac{\partial \eta}{\partial X_3} & \frac{\partial \zeta}{\partial X_3} & \frac{\partial \xi}{\partial X_2} & \frac{\partial \eta}{\partial X_2} & \frac{\partial \zeta}{\partial X_2} \\ \frac{\partial \xi}{\partial X_3} & \frac{\partial \eta}{\partial X_3} & \frac{\partial \zeta}{\partial X_3} & 0 & 0 & 0 & \frac{\partial \xi}{\partial X_1} & \frac{\partial \eta}{\partial X_1} & \frac{\partial \zeta}{\partial X_1} \end{bmatrix}, \quad (15)$$

$$\hat{\mathbf{B}}_{\text{lin}} = \begin{bmatrix} \mathbf{A}_{\text{lin}} & \mathbf{0} & \mathbf{0} \\ \mathbf{0} & \mathbf{A}_{\text{lin}} & \mathbf{0} \\ \mathbf{0} & \mathbf{0} & \mathbf{A}_{\text{lin}} \end{bmatrix} \quad \text{with} \quad \mathbf{A}_{\text{lin}} = \begin{bmatrix} 0 & 1 & 0 & 0 \\ 0 & 0 & 1 & 0 \\ 0 & 0 & 0 & 1 \end{bmatrix} \quad (16)$$

and

$$\hat{\mathbf{B}}_{\text{hg}} = \begin{bmatrix} \mathbf{A}_{\text{hg}} & \mathbf{0} & \mathbf{0} \\ \mathbf{0} & \mathbf{A}_{\text{hg}} & \mathbf{0} \\ \mathbf{0} & \mathbf{0} & \mathbf{A}_{\text{hg}} \end{bmatrix} \quad \text{with} \quad \mathbf{A}_{\text{hg}} = \begin{bmatrix} \eta & 0 & \zeta & \eta \zeta \\ \xi & \zeta & 0 & \zeta \xi \\ 0 & \eta & \xi & \xi \eta \end{bmatrix}. \quad (17)$$

The  $12 \times 24$ -matrices  $\mathbf{M}_{\text{lin}}$  and  $\mathbf{M}_{\text{hg}}$  are defined as follows:

$$\mathbf{M}_{\text{lin}}^T = \begin{bmatrix} \mathbf{Z}_{\text{lin}} & \mathbf{0} & \mathbf{0} \\ \mathbf{0} & \mathbf{Z}_{\text{lin}} & \mathbf{0} \\ \mathbf{0} & \mathbf{0} & \mathbf{Z}_{\text{lin}} \end{bmatrix} \quad \text{with} \quad \mathbf{Z}_{\text{lin}} = [ \mathbf{0} \quad \mathbf{b}_1 \quad \mathbf{b}_2 \quad \mathbf{b}_3 ] \quad (18)$$

$$\mathbf{M}_{\text{hg}}^T = \begin{bmatrix} \mathbf{Z}_{\text{hg}} & \mathbf{0} & \mathbf{0} \\ \mathbf{0} & \mathbf{Z}_{\text{hg}} & \mathbf{0} \\ \mathbf{0} & \mathbf{0} & \mathbf{Z}_{\text{hg}} \end{bmatrix} \quad \text{with} \quad \mathbf{Z}_{\text{hg}} = \begin{bmatrix} \gamma_{\xi\eta} & \gamma_{\eta\zeta} & \gamma_{\zeta\xi} & \gamma_{\xi\eta\zeta} \end{bmatrix} \quad (19)$$

Using further the argument that the variations in (9) are arbitrary and no continuity over the element boundaries is required for  $\boldsymbol{\varepsilon}_{\text{enh}}^h$  we derive the relation

$$\int_{\mathcal{B}_{0e}^h} (\delta \boldsymbol{\varepsilon}_{\text{enh}}^h)^T \mathcal{C}_0 (\boldsymbol{\varepsilon}_{\text{comp}}^h + \boldsymbol{\varepsilon}_{\text{enh}}^h) dV_e^h = 0 \quad (20)$$

which yields with  $\mathcal{K} = \mathbf{j}^T \mathcal{C}_0 \mathbf{j}$  after inserting the interpolation functions

$$\begin{aligned} \delta \mathbf{p}^T \left( \int_{\mathcal{B}_{0e}^h} \hat{\mathbf{G}}^T \mathcal{K} \hat{\mathbf{G}} dV_e^h \mathbf{p} + \int_{\mathcal{B}_{0e}^h} \hat{\mathbf{G}}^T \mathcal{K} \hat{\mathbf{B}}_{\text{lin}} dV_e^h \mathbf{M}_{\text{lin}} \mathbf{d} \right. \\ \left. + \int_{\mathcal{B}_{0e}^h} \hat{\mathbf{G}}^T \mathcal{K} \hat{\mathbf{B}}_{\text{hg}} dV_e^h \mathbf{M}_{\text{hg}} \mathbf{d} \right) = 0. \end{aligned} \quad (21)$$

At this point, we exploit the notion of the equivalent parallelepiped which is assumed to be the analogue to the equivalent parallelogram derived by Arunakirithanar and Reddy<sup>16,17</sup>. The latter authors showed that the error in evaluating quantities on the equivalent parallelogram rather than on the actual quadrilateral is of the order of mesh size, and goes to zero with increasing number of elements. Computing above expression on the equivalent parallelepiped leads to

$$\mathbf{K}_{pp} \mathbf{p} + \mathbf{K}_{pd} \mathbf{M}_{\text{hg}} \mathbf{d} = \mathbf{0} \quad \Rightarrow \quad \mathbf{p} = -\mathbf{K}_{pp}^{-1} \mathbf{K}_{pd} \mathbf{M}_{\text{hg}} \mathbf{d}, \quad (22)$$

where the short hand notations

$$\mathbf{K}_{pp} = \int_{\mathcal{B}_{0e}^h} \hat{\mathbf{G}}^T \mathcal{K}_0 \hat{\mathbf{G}} dV_{e0}^h, \quad \mathbf{K}_{pd} = \int_{\mathcal{B}_{0e}^h} \hat{\mathbf{G}}^T \mathcal{K}_0 \hat{\mathbf{B}}_{\text{hg}} dV_{e0}^h, \quad (23)$$

$\mathbf{p}^T = \{\mathbf{p}_1^T, \mathbf{p}_2^T, \mathbf{p}_3^T\}$  and  $\mathbf{d}^T = \{\mathbf{d}_1^T, \mathbf{d}_2^T, \mathbf{d}_3^T\}$  have been used. Note that we could have produced this result also by evaluating  $\mathbf{j}$  and  $dV_e^h$  in the center of the element. Using

$$\mathbf{K}_{e0} = \int_{\mathcal{K}_{0e}^h} \hat{\mathbf{B}}_{\text{lin}}^T \mathcal{K}_0 \hat{\mathbf{B}}_{\text{lin}} dV_{e0}^h \quad (24)$$

and inserting (23) in (9) gives finally

$$\begin{aligned} g_{\text{enh}}^l &= \sum_{e=1}^{n_e} \delta \mathbf{d}^T \left( \mathbf{K}_{e0} + \mathbf{M}_{\text{hg}}^T \underbrace{\int_{\mathcal{B}_{0e}^h} \hat{\mathbf{B}}_{\text{enh}}^T \mathcal{K}_0 \hat{\mathbf{B}}_{\text{enh}} dV_{e0}^h}_{\mathbf{K}_{\text{stab}}} \mathbf{M}_{\text{hg}} \right) \mathbf{d} - g_a \\ &= \sum_{e=1}^{n_e} \delta \mathbf{d}^T \left( \mathbf{K}_{e0} + \mathbf{K}_{e\text{hg}} \right) \mathbf{d} - g_a = 0, \end{aligned} \quad (25)$$

where the matrix  $\hat{\mathbf{B}}_{\text{enh}}$  is defined by

$$\hat{\mathbf{B}}_{\text{enh}} = \hat{\mathbf{B}}_{\text{hg}} - \hat{\mathbf{G}} \mathbf{K}_{pp}^{-1} \mathbf{K}_{pd}. \quad (26)$$

The matrix  $\mathbf{K}_{e0}$  is the part of the stiffness matrix which would be obtained, if only a pure one Gauss point integration was carried out. This part does not contribute to locking and thus remains the same as in the standard displacement formulation. The stabilization part, however, is different due to the term  $\hat{\mathbf{G}} \mathbf{K}_{pp}^{-1} \mathbf{K}_{pd}$  resulting from employing the enhanced strain method. Note that the stabilization matrix can be evaluated analytically; i.e. an numerical integration is here avoided completely.

It has already been observed by Wilson et al.<sup>21</sup> that due to the bilinear terms  $\xi \eta$ ,  $\eta \zeta$  and  $\zeta \xi$  in (7) still mild volumetric locking occurs. A simple possibility to avoid also this effect, is to modify  $\mathbf{B}$  as follows:

$$\mathbf{B} = \mathbf{j} (\hat{\mathbf{B}}_{\text{lin}} \mathbf{M}_{\text{lin}} + \hat{\mathbf{B}}_{\text{hg}1} \mathbf{M}_{\text{hg}}) + \mathbf{j}_2 \hat{\mathbf{B}}_{\text{hg}2} \mathbf{M}_{\text{hg}} \quad (27)$$

with

$$\hat{\mathbf{B}}_{\text{hg}1} = \begin{bmatrix} \mathbf{A}_{\text{hg}1} & \mathbf{0} & \mathbf{0} \\ \mathbf{0} & \mathbf{A}_{\text{hg}1} & \mathbf{0} \\ \mathbf{0} & \mathbf{0} & \mathbf{A}_{\text{hg}1} \end{bmatrix}; \quad \mathbf{A}_{\text{hg}1} = \begin{bmatrix} \eta & 0 & \zeta & 0 \\ \xi & \zeta & 0 & 0 \\ 0 & \eta & \xi & 0 \end{bmatrix} \quad (28)$$

$$\hat{\mathbf{B}}_{\text{hg}2} = \begin{bmatrix} \mathbf{A}_{\text{hg}2} & \mathbf{0} & \mathbf{0} \\ \mathbf{0} & \mathbf{A}_{\text{hg}2} & \mathbf{0} \\ \mathbf{0} & \mathbf{0} & \mathbf{A}_{\text{hg}2} \end{bmatrix}; \quad \mathbf{A}_{\text{hg}2} = \begin{bmatrix} 0 & 0 & 0 & \sqrt{3} \eta \zeta \\ 0 & 0 & 0 & \sqrt{3} \zeta \xi \\ 0 & 0 & 0 & \sqrt{3} \xi \eta \end{bmatrix} \quad (29)$$

and

$$\mathbf{j}_2 = \begin{bmatrix} 0 & 0 & 0 & 0 & 0 & 0 & 0 & 0 & 0 \\ 0 & 0 & 0 & 0 & 0 & 0 & 0 & 0 & 0 \\ 0 & 0 & 0 & 0 & 0 & 0 & 0 & 0 & 0 \\ \frac{\partial \xi}{\partial X_2} & \frac{\partial \eta}{\partial X_2} & \frac{\partial \zeta}{\partial X_2} & \frac{\partial \xi}{\partial X_1} & \frac{\partial \eta}{\partial X_1} & \frac{\partial \zeta}{\partial X_1} & 0 & 0 & 0 \\ 0 & 0 & 0 & \frac{\partial \xi}{\partial X_3} & \frac{\partial \eta}{\partial X_3} & \frac{\partial \zeta}{\partial X_3} & \frac{\partial \xi}{\partial X_2} & \frac{\partial \eta}{\partial X_2} & \frac{\partial \zeta}{\partial X_2} \\ \frac{\partial \xi}{\partial X_3} & \frac{\partial \eta}{\partial X_3} & \frac{\partial \zeta}{\partial X_3} & 0 & 0 & 0 & \frac{\partial \xi}{\partial X_1} & \frac{\partial \eta}{\partial X_1} & \frac{\partial \zeta}{\partial X_1} \end{bmatrix} \quad (30)$$

This kind of interpolation has already been applied by Korelc and Wriggers<sup>19</sup>. It goes without saying, that the matrices are sparse and can therefore be coded in a very efficient way. The factor  $\sqrt{3}$  in  $\hat{\mathbf{B}}_{\text{hg}2}$  is needed to obtain the same eigenvalues as e.g. reported in Simo et al.<sup>3</sup>. A stabilization concept equivalent to the QS/E9 element developed by Korelc and Wriggers<sup>19</sup> is derived by simply leaving out the factor  $\sqrt{3}$ . Then, however, one does not compute the correct eigenvalues. If the factor is taken into account we recover a stabilization version of the linear QM1/E12 element. Note that the results of the present method are absolutely identical to those of the according mixed method, if the calculation is based on an undistorted element geometry.

### 3.2 Hourglass stabilization in the large deformation case

The preceding derivations might not have been presented before in such a form but have already been discussed in one way or the other by several authors (see besides the already mentioned Hacker and Schreyer<sup>23</sup>, Hueck and Wriggers<sup>24</sup>, Küssner and Reddy<sup>18</sup>). All these papers, however, deal exclusively with the small deformation case. For large deformation problems, interestingly, the stabilization method did not attract much attention which is in the opinion of the authors mainly due to the fact that an equivalence with a mixed method is difficult to find. Note again that such an equivalence is necessary to derive the stabilization factors. There is no doubt that a formulation which requires to choose these factors arbitrarily cannot be considered as a serious alternative to the already existing non-linear element formulations. Thus, it is our first task here to search for an appropriate equivalent principle which lets us then derive the stabilization factors in such a way that locking is avoided.

#### 3.2.1 Computation of the stabilization factors

It is well-known that in the range of small deformations, enhanced strain elements behave extraordinarily well. Then, it is absolutely satisfactory to develop a stabilization method which recovers these results. In the case of large deformations, the situation is different, since the performance of the enhanced strain method in compression tests is not acceptable and therefore should not be reproduced by the new element. This fact led Reese et al.<sup>15</sup> to the conclusion that the computation of the stabilization factors is reasonably based on a *linearized* form of the Hu-Washizu principle, where the geometrical part of the stiffness is left out to ensure stability. The present work now shows that this might lead to mild locking in shell problems. For this reason, we represent here the stabilization concept in a new version with the stabilization based on the full tangent. This formulation requires to work with nine-dimensional tangent matrices. Note that the switch to the original method is trivial and for example carried out to guarantee stable behaviour in the compression of a block.

Applying the non-linear Hu-Washizu principle leads after several steps to the weak form

$$\begin{aligned} g_{\text{enh}} &= \hat{g}_{\text{enh}}(\mathbf{u}^h, \delta \mathbf{u}^h, \mathbf{H}_{\text{enh}}^h, \delta \mathbf{H}_{\text{enh}}^h) \\ &= \int_{B_0^h} (\delta \mathbf{H}_{\text{comp}}^h + \delta \mathbf{H}_{\text{enh}}^h)^T \frac{\partial W^h}{\partial \mathbf{H}^h} dV^h - \hat{g}_a(\delta \mathbf{u}^h) = 0, \end{aligned} \quad (31)$$

where the total displacement gradient  $\mathbf{H}^h$  is split in a compatible part  $\mathbf{H}_{\text{comp}}^h = \text{Grad } \mathbf{u}^h$  and an enhanced or incompatible part  $\mathbf{H}_{\text{enh}}^h$  (see Simo and Armero<sup>2</sup> for more details). Using matrix notation,  $\mathbf{H}^h$  is represented as a nine-dimensional vector. The solution of the non-linear equation (31) is usually carried out by applying Newton's method which requires to solve the linearized equation  $\Delta(g_{\text{enh}})_i = -(g_{\text{enh}})_{i-1}$  in each iteration step  $i$  till the weak form (31) is fulfilled with sufficient tolerance.  $\Delta g_{\text{enh}}$  is a short hand notation for the Gateaux

derivative of  $g_{\text{enh}}$  determined by the expression

$$\begin{aligned} \Delta g_{\text{enh}} &= \int_{\mathcal{B}_0^h} (\delta \mathbf{H}_{\text{comp}}^h + \delta \mathbf{H}_{\text{enh}}^h)^T \mathcal{A}^h (\Delta \mathbf{H}_{\text{comp}}^h + \Delta \mathbf{H}_{\text{enh}}^h) dV^h \quad (32) \\ &= \int_{\mathcal{B}_t^h} (\delta \mathbf{h}_{\text{comp}}^h + \delta \mathbf{h}_{\text{enh}}^h)^T (\mathcal{C}^h + \mathcal{D}^h) (\Delta \mathbf{h}_{\text{comp}}^h + \Delta \mathbf{h}_{\text{enh}}^h) dv^h. \end{aligned}$$

In the latter relation, the nine-dimensional matrix  $\mathcal{A}^h$  is given by

$$\mathcal{A}^h = \frac{\partial^2 W}{\partial \mathbf{H}^h \partial \mathbf{H}^h}. \quad (33)$$

The second line (32)<sub>2</sub> is obtained by pushing (32)<sub>1</sub> forward to the current configuration and splitting the resulting tangent matrix in the material part  $\mathcal{C}^h$  and the geometrical part  $\mathcal{D}^h$ . This split is easily explained by looking at the relation

$$\frac{1}{J} F_{ja} A_{iakb} F_{lb} = C_{ijkl} + \sigma_{jl} \delta_{ik} = C_{ijkl} + D_{ijkl}, \quad (34)$$

where the quantities  $F_{..}$ ,  $A_{...}$ ,  $C_{...}$ ,  $D_{...}$  and  $\sigma_{..}$  represent the coefficients of the tensors  $\mathbf{F}$ ,  $\mathbf{A}$ ,  $\mathbf{C}$ ,  $\mathbf{D}$  and  $\boldsymbol{\sigma}$ , respectively. Here,  $\mathbf{F}$  is the deformation gradient and  $\boldsymbol{\sigma}$  denotes the Cauchy stress tensor. Note further that the fourth order tensors  $\mathbf{C}^h$  and  $\mathbf{D}^h$  are not symmetric neither with respect to the first two nor with respect to the last two indices. For this reason, the matrices  $\mathcal{C}^h$  and  $\mathcal{D}^h$  obtained from writing  $\mathbf{C}^h$  and  $\mathbf{D}^h$  in matrix form must be nine-dimensional. The quantity  $J$  is a short hand notation for the determinant of the deformation gradient and is needed for the computation of the volume element with respect to the current configuration  $dv^h = J^h dV^h$ . The quantities  $\Delta \mathbf{h}_{\text{comp}}^h$  and  $\Delta \mathbf{h}_{\text{enh}}^h$  denote vector representations of the strain tensor increments

$$\Delta \mathbf{h}_{\text{comp}}^h := \Delta \mathbf{H}_{\text{comp}}^h \cdot (\mathbf{F}^h)^{-1} \quad (35)$$

$$\Delta \mathbf{h}_{\text{enh}}^h := \Delta \mathbf{H}_{\text{enh}}^h \cdot (\mathbf{F}^h)^{-1} \quad (36)$$

It is now not difficult to see that we have derived a form analogous to the relation (9), upon which the computation of the stabilization factors in the small deformation case has been based. Due to this analogy, the calculation of the stabilization factors can be carried out in a way which is very similar to the procedure in linear elasticity. The differences are summarized in the following paragraph:

- 1.) The strain increments (35) and (36) are not symmetric. This requires a nine-dimensional vector representation resulting in a slight modification (see equation (37)) of the matrices  $\mathbf{j}$  (15) and  $\mathbf{j}_2$  (30) in the linear case.
- 2.) The strain increments  $\Delta \mathbf{h}_{\text{comp}}^h$  and  $\Delta \mathbf{h}_{\text{enh}}^h$  are related to the deformed configuration. Thus, the partial derivatives in  $\mathbf{j}$  and  $\mathbf{j}_2$  have to be formulated

with respect to the spatial coordinates  $x_1$ ,  $x_2$  and  $x_3$ :

$$\mathbf{j} = \begin{bmatrix} \frac{\partial \xi}{\partial x_1} & \frac{\partial \eta}{\partial x_1} & \frac{\partial \zeta}{\partial x_1} & 0 & 0 & 0 & 0 & 0 & 0 \\ 0 & 0 & 0 & \frac{\partial \xi}{\partial x_2} & \frac{\partial \eta}{\partial x_2} & \frac{\partial \zeta}{\partial x_2} & 0 & 0 & 0 \\ 0 & 0 & 0 & 0 & 0 & 0 & \frac{\partial \xi}{\partial x_3} & \frac{\partial \eta}{\partial x_3} & \frac{\partial \zeta}{\partial x_3} \\ \frac{\partial \xi}{\partial x_2} & \frac{\partial \eta}{\partial x_2} & \frac{\partial \zeta}{\partial x_2} & 0 & 0 & 0 & 0 & 0 & 0 \\ 0 & 0 & 0 & \frac{\partial \xi}{\partial x_1} & \frac{\partial \eta}{\partial x_1} & \frac{\partial \zeta}{\partial x_1} & 0 & 0 & 0 \\ 0 & 0 & 0 & \frac{\partial \xi}{\partial x_3} & \frac{\partial \eta}{\partial x_3} & \frac{\partial \zeta}{\partial x_3} & 0 & 0 & 0 \\ 0 & 0 & 0 & 0 & 0 & 0 & \frac{\partial \xi}{\partial x_2} & \frac{\partial \eta}{\partial x_2} & \frac{\partial \zeta}{\partial x_2} \\ 0 & 0 & 0 & 0 & 0 & 0 & \frac{\partial \xi}{\partial x_1} & \frac{\partial \eta}{\partial x_1} & \frac{\partial \zeta}{\partial x_1} \\ \frac{\partial \xi}{\partial x_3} & \frac{\partial \eta}{\partial x_3} & \frac{\partial \zeta}{\partial x_3} & 0 & 0 & 0 & 0 & 0 & 0 \end{bmatrix} \quad (37)$$

( $\mathbf{j}_2$  is modified accordingly). Further, also the equivalent parallelepiped is based on spatial coordinates.

- 3.) The ‘‘tangent’’ matrices  $\mathcal{C}^h$  and  $\mathcal{D}^h$  are not constant over the element. This could be taken into account in the calculation of the stabilization factors. For the purpose of maintaining the simplicity of the element formulation, we evaluate these quantities only in the center of the element. Note that this represents a further approximation.

### 3.2.2 Weak form

It should be stated very clearly that the preceding derivation serves *only* for the calculation of the stabilization factors. The element formulation itself, however, is a classical stabilization concept and as such based on reduced integration plus stabilization of the standard weak formulation (5). Only then, we can utilize the equality  $\text{grad } \mathbf{u}^h = \text{Grad } \mathbf{u}^h \cdot (\mathbf{F}^h)^{-1}$ . In an enhanced strain concept, however, the deformation gradient would additionally include the incompatible strain tensor  $\mathbf{H}_{\text{enh}}^h$ .

Let us summarize the main steps of the stabilization technique in the context of large deformations. Employing Newton’s method on (5) yields the iteration algorithm

$$\begin{aligned} \left[ \int_{\mathcal{B}_i^h} (\delta \mathbf{h}^h)^T (\mathcal{C}^h + \mathcal{D}^h) \Delta \mathbf{h}^h dv^h \right]_i &= - \left[ \int_{\mathcal{B}_i^h} (\delta \mathbf{h}^h)^T \boldsymbol{\sigma}^h dv^h \right]_{i-1} \\ \mathbf{u}_i^h &= \mathbf{u}_{i-1}^h + \Delta \mathbf{u}_i^h \\ i-1 &\leftarrow i \end{aligned} \quad (38)$$

The integral on the left side of (38)<sub>1</sub> is computed by means of

$$\int_{\mathcal{B}_i^h} (\delta \mathbf{h}^h)^T (\mathcal{C}^h + \mathcal{D}^h) \Delta \mathbf{h}^h dv^h = \sum_{e=1}^{n_e} \delta \mathbf{d}^T \left( \mathbf{K}_0 + \mathbf{K}_{\text{hg}} \right) \Delta \mathbf{d}, \quad (39)$$

where we determine the matrices  $\mathbf{K}_{e0}$  and  $\mathbf{K}_{e\text{hg}}$  in the same way as shown in Section 3.1 but on the basis of  $(32)_2$ . Under the assumption that the stabilization factors are held constant during the iteration, the right hand side of  $(38)_1$  takes the form

$$\int_{B_i^h} (\delta \mathbf{h}^h)^T \boldsymbol{\sigma}^h dv^h = \sum_{e=1}^{n_e} \delta \mathbf{d}^T \left( \mathbf{G}_{e0} + \mathbf{K}_{e\text{hg}} \mathbf{d} \right). \quad (40)$$

In the latter equation, the vector  $\mathbf{G}_{e0} = \mathbf{R}_{e0} - \mathbf{P}_e$  consists of the vector of inner forces evaluated in the center of the element  $\mathbf{R}_{e0}$  and the load vector on element level  $\mathbf{P}_e$ .

If the stabilization factors were updated in every iteration we would lose the crucial property of quadratic convergence to the solution. On the other hand, holding the stabilization factors constant within one load increment results in a solution which is dependent on the size of the load increment chosen. Note that this load step dependency has purely numerical character and would certainly represent a drawback of such a stabilization procedure.

In order to circumvent the problem, we proceed in the following way. The stabilization factors are determined in the first iteration step and then held constant till the weak form is fulfilled. Then, we update the factors and employ the iteration procedure  $(38)$  again. If the results are relatively independent of the size of the load increment, usually one after-iteration is sufficient to achieve practically converged results. This is e. g. the case for the examples presented in Reese et al.<sup>15</sup>. Several after-iterations, however, are necessary to model the bending of thin shell structures.

As already shown in Section 3.1,  $\mathbf{K}_{e\text{hg}}$  is computed by means of  $\mathbf{K}_{e\text{hg}} = \mathbf{M}_{\text{hg}}^T \mathbf{K}_{\text{stab}} \mathbf{M}_{\text{hg}}$ , where  $\mathbf{K}_{\text{stab}}$  has the following form:

$$\mathbf{K}_{\text{stab}} = \underbrace{\begin{bmatrix} \bullet & \bullet & \bullet & 0 & \bullet & \bullet & \bullet & 0 & \bullet & \bullet & \bullet & 0 \\ \bullet & \bullet & \bullet & 0 & \bullet & \bullet & \bullet & 0 & \bullet & \bullet & \bullet & 0 \\ \bullet & \bullet & \bullet & 0 & \bullet & \bullet & \bullet & 0 & \bullet & \bullet & \bullet & 0 \\ 0 & 0 & 0 & 0 & 0 & 0 & 0 & 0 & 0 & 0 & 0 & 0 \\ \bullet & \bullet & \bullet & 0 & \bullet & \bullet & \bullet & 0 & \bullet & \bullet & \bullet & 0 \\ \bullet & \bullet & \bullet & 0 & \bullet & \bullet & \bullet & 0 & \bullet & \bullet & \bullet & 0 \\ \bullet & \bullet & \bullet & 0 & \bullet & \bullet & \bullet & 0 & \bullet & \bullet & \bullet & 0 \\ 0 & 0 & 0 & 0 & 0 & 0 & 0 & 0 & 0 & 0 & 0 & 0 \\ \bullet & \bullet & \bullet & 0 & \bullet & \bullet & \bullet & 0 & \bullet & \bullet & \bullet & 0 \\ \bullet & \bullet & \bullet & 0 & \bullet & \bullet & \bullet & 0 & \bullet & \bullet & \bullet & 0 \\ \bullet & \bullet & \bullet & 0 & \bullet & \bullet & \bullet & 0 & \bullet & \bullet & \bullet & 0 \\ 0 & 0 & 0 & 0 & 0 & 0 & 0 & 0 & 0 & 0 & 0 & 0 \end{bmatrix}}_{\mathbf{K}_{\text{stab}1}} + \dots$$

$$\dots + \underbrace{\begin{bmatrix} 0 & 0 & 0 & 0 & 0 & 0 & 0 & 0 & 0 & 0 & 0 & 0 & 0 \\ 0 & 0 & 0 & 0 & 0 & 0 & 0 & 0 & 0 & 0 & 0 & 0 & 0 \\ 0 & 0 & 0 & 0 & 0 & 0 & 0 & 0 & 0 & 0 & 0 & 0 & 0 \\ 0 & 0 & 0 & \bullet & 0 & 0 & 0 & \bullet & 0 & 0 & 0 & \bullet & 0 \\ 0 & 0 & 0 & 0 & 0 & 0 & 0 & 0 & 0 & 0 & 0 & 0 & 0 \\ 0 & 0 & 0 & 0 & 0 & 0 & 0 & 0 & 0 & 0 & 0 & 0 & 0 \\ 0 & 0 & 0 & 0 & 0 & 0 & 0 & 0 & 0 & 0 & 0 & 0 & 0 \\ 0 & 0 & 0 & 0 & 0 & 0 & 0 & 0 & 0 & 0 & 0 & 0 & 0 \\ 0 & 0 & 0 & 0 & 0 & 0 & 0 & 0 & 0 & 0 & 0 & 0 & 0 \\ 0 & 0 & 0 & 0 & 0 & 0 & 0 & 0 & 0 & 0 & 0 & 0 & 0 \\ 0 & 0 & 0 & \bullet & 0 & 0 & 0 & \bullet & 0 & 0 & 0 & \bullet & 0 \\ 0 & 0 & 0 & 0 & 0 & 0 & 0 & 0 & 0 & 0 & 0 & 0 & 0 \\ 0 & 0 & 0 & 0 & 0 & 0 & 0 & 0 & 0 & 0 & 0 & 0 & 0 \\ 0 & 0 & 0 & 0 & 0 & 0 & 0 & 0 & 0 & 0 & 0 & 0 & 0 \\ 0 & 0 & 0 & \bullet & 0 & 0 & 0 & \bullet & 0 & 0 & 0 & \bullet & 0 \end{bmatrix}}_{\mathbf{K}_{\text{stab } 2}} \quad (41)$$

The decoupled structure reduces the number of stabilization parameters to be stored for the next iteration noticeably. Due to the symmetry of the stabilization matrix, there are 51 independent stabilization factors. This is already much less than the 354 history variables necessary for the QM1/E12 element developed by Simo et al.<sup>3</sup> who derived an internal iteration procedure in order to reduce this number. In this way, only the twelve internal degrees of freedom remain in the history field. Note that in the present element formulation, the storage of any variables can be simply avoided by a recalculation of the stabilization parameters in every iteration.

To conclude, let us say some words about stability. It is beyond question that a well-behaved element should not exhibit any non-physical instabilities as it is unfortunately the case for most enhanced strain elements. In order to check the present formulation, we discuss possible solutions of the eigenvalue problem

$$\underbrace{(\mathbf{K}_{e0} + \mathbf{K}_{e \text{ hg}} - \omega \mathbf{1}^{24})}_{\mathbf{K}_e} \boldsymbol{\varphi}_e = \mathbf{0}. \quad (42)$$

Let us further assume that the element under investigation has the form of a parallelepiped. It should be kept in mind that this is actually the case in the limit of an infinitely fine discretization. The stabilization vectors then reduce to the associated “hourglass” vectors, i.e. we have  $\boldsymbol{\gamma}_{\xi\eta} = \mathbf{h}_{\xi\eta}$ ,  $\boldsymbol{\gamma}_{\eta\zeta} = \mathbf{h}_{\eta\zeta}$ ,  $\boldsymbol{\gamma}_{\zeta\xi} = \mathbf{h}_{\zeta\xi}$ ,  $\boldsymbol{\gamma}_{\xi\eta\zeta} = \mathbf{h}_{\xi\eta\zeta}$ . Note that the hourglass vectors are orthogonal to  $\mathbf{b}_i$  ( $i = 1, 2, 3$ ). Using the relation  $\mathbf{K}_e = \mathbf{M}^T (\tilde{\mathbf{K}}_0 + \tilde{\mathbf{K}}_{\text{stab}}) \mathbf{M}$  and the orthogonality of

$$\mathbf{M}^T = \begin{bmatrix} 0 & \mathbf{b}_1 & \mathbf{b}_2 & \mathbf{b}_3 & \mathbf{h}_{\xi\eta} & \mathbf{h}_{\eta\zeta} & \mathbf{h}_{\zeta\xi} & \mathbf{h}_{\xi\eta\zeta} & 0 & 0 & 0 & 0 \\ 0 & 0 & 0 & 0 & 0 & 0 & 0 & 0 & 0 & \mathbf{b}_1 & \mathbf{b}_2 & \mathbf{b}_3 \\ 0 & 0 & 0 & 0 & 0 & 0 & 0 & 0 & 0 & 0 & 0 & 0 \\ 0 & 0 & 0 & 0 & 0 & 0 & 0 & 0 & 0 & 0 & 0 & 0 \\ \mathbf{h}_{\xi\eta} & \mathbf{h}_{\eta\zeta} & \mathbf{h}_{\zeta\xi} & \mathbf{h}_{\xi\eta\zeta} & 0 & 0 & 0 & 0 & 0 & 0 & 0 & 0 \\ 0 & 0 & 0 & 0 & 0 & \mathbf{b}_1 & \mathbf{b}_2 & \mathbf{b}_3 & \mathbf{h}_{\xi\eta} & \mathbf{h}_{\eta\zeta} & \mathbf{h}_{\zeta\xi} & \mathbf{h}_{\xi\eta\zeta} \end{bmatrix}$$

we may alternatively to (42) investigate the eigenvalue problem

$$\underbrace{(\hat{\mathbf{K}}_0 + \hat{\mathbf{K}}_{\text{stab}})}_{\hat{\mathbf{K}}} - \omega \mathbf{1}^{24}) (\mathbf{M} \boldsymbol{\varphi}_e) = \mathbf{0}, \quad (43)$$

where  $\hat{\mathbf{K}}$  is a 24-dimensional matrix with the following interesting structure:

$$\hat{\mathbf{K}} = \begin{bmatrix} \bullet & \mathbf{0} & \bullet & \mathbf{0} & \bullet & \mathbf{0} \\ \mathbf{0} & \times & \mathbf{0} & \times & \mathbf{0} & \times \\ \bullet & \mathbf{0} & \bullet & \mathbf{0} & \bullet & \mathbf{0} \\ \mathbf{0} & \times & \mathbf{0} & \times & \mathbf{0} & \times \\ \bullet & \mathbf{0} & \bullet & \mathbf{0} & \bullet & \mathbf{0} \\ \mathbf{0} & \times & \mathbf{0} & \times & \mathbf{0} & \times \end{bmatrix} \quad (44)$$

Note that  $\bullet$  stands here for the contributions of  $\hat{\mathbf{K}}_0$ , whereas  $\times$  characterizes the coefficients of  $\hat{\mathbf{K}}_{\text{stab}}$ . If we additionally assume that  $\boldsymbol{\varphi}_e$  is a hourglass eigenvector, then, due to  $\mathbf{b}_i^T \mathbf{h}_{\dots} = 0$ , the eigenvector  $\mathbf{M} \boldsymbol{\varphi}_e$  appears as

$$(\mathbf{M} \boldsymbol{\varphi}_e)_{\text{hg}}^T = \{\mathbf{0}^T, \times, \mathbf{0}^T, \times, \mathbf{0}^T, \times\}, \quad (45)$$

where  $\times$  marks the coefficients which are not zero. Inserting  $\mathbf{M} \boldsymbol{\varphi}_e$  in the eigenvalue problem in the above shows immediately that (43) reduces to

$$(\hat{\mathbf{K}}_{\text{stab}} - \omega \mathbf{1}^{24}) (\mathbf{M} \boldsymbol{\varphi}_e)_{\text{hg}} = \mathbf{0} \quad (46)$$

Thus, in order to exclude the possibility that pure hourglass eigenforms arise, the stabilization matrix  $\hat{\mathbf{K}}_{\text{stab}}$  has to remain positive definite!

In the context of the present formulation, such a stability check could be carried out easily e. g. by solving an eigenvalue problem for the stabilization matrix  $\hat{\mathbf{K}}_{\text{stab}}$  and resetting any problematic factors. The enhanced strain method, however, for which the preceding derivation would hold in an analogous way, is much less flexible in this regard which can be considered as one of its main disadvantages.

## 4 Examples

In order to validate the present approach, we investigate two demanding examples belonging to two important classes of problems. The first concerns the bending of shells. In the second, the compression of a nearly incompressible block is investigated. As in Reese et al.<sup>15</sup>, we use the abbreviation Q1SP for the new element, where Q1 stands for the standard bilinear interpolation of the displacement degrees of freedom, S refers to stabilization and P indicates the important role of the equivalent parallelepiped.

## 4.1 Cylindric shell

Shell elements which are appropriate for the present example are highly sophisticated and therefore not very efficient. For this reason, one would prefer the implementation of a brick element, if one could achieve comparable results. Geometry, boundary conditions, loading and deformed configuration of the system are shown in Figure 1. Only one quarter of the whole structure is discretized and shown in the plot. The boundary conditions on the planes  $X_3 = 0$  and  $X_1 = 0$  are set accordingly. The material model is a compressible Neo-Hooke model with the strain energy function  $W = \frac{\mu}{2} (\mathbf{b} - \mathbf{1}) - \mu \ln J + \frac{\Lambda}{2} (\ln J)^2$  ( $\mathbf{b}$  left Cauchy-Green tensor) and the material parameters  $\mu = 6000 \text{ N/mm}^2$  and  $\Lambda = 240000 \text{ N/mm}^2$ .

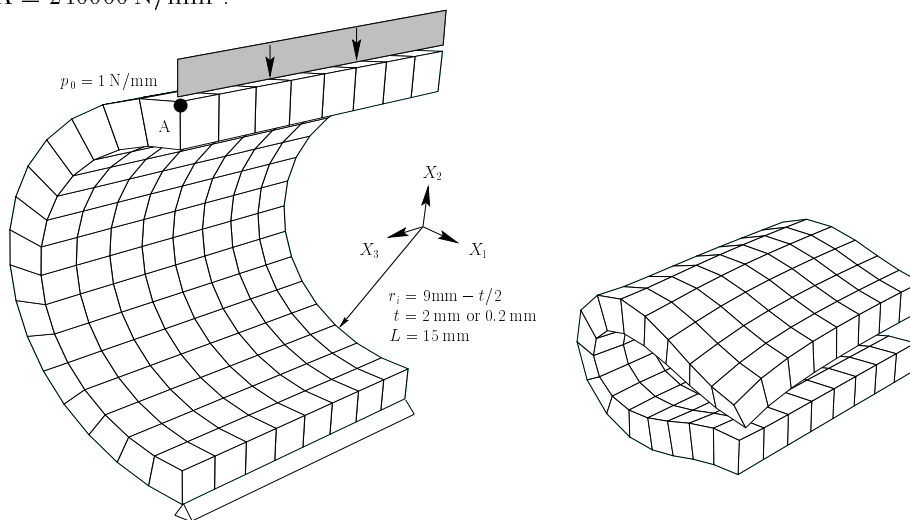


Figure 1: Cylindric shell

A study of convergence has been carried out for a moderately thick shell with  $t = 2 \text{ mm}$  ( $\nu = p/p_0 = 7500$ ) and a thin shell with  $t = 0.2 \text{ mm}$  ( $\nu = 8.5$ ). The results of various element formulations are plotted in Figure 2. Three different discretizations have been tested ( $1 \times 8 \times 4$ ,  $1 \times 16 \times 8$ ,  $1 \times 32 \times 16$ ). It should be emphasized that only one element over the thickness is necessary to model the bending behaviour. Among the brick elements, only QM1/E12 and Q1SP show a satisfying convergence to the correct solution. The standard displacement element formulation Q1 and also the non-linear B-Bar method Q1/P0 do not perform satisfactorily which is in particular visible for the thin shell problem. Excellent results, especially for the thin shell, can be achieved with sophisticated shell formulations as the ones of Büchter et al.<sup>25</sup> or Eberlein and Wriggers<sup>26</sup> (see “SHELL” in Figure 2). Thus, we can conclude that Q1SP shows very convincing results and a surprising robustness in this extreme bending situation. The performance is comparable if not better than that of the QM1/E12 element which behaves usually extraordinarily well for such kind of problems. It should

not be concealed, however, that just for the thin shell, several after-iterations (updates of the stabilization factors) are necessary to achieve these results.

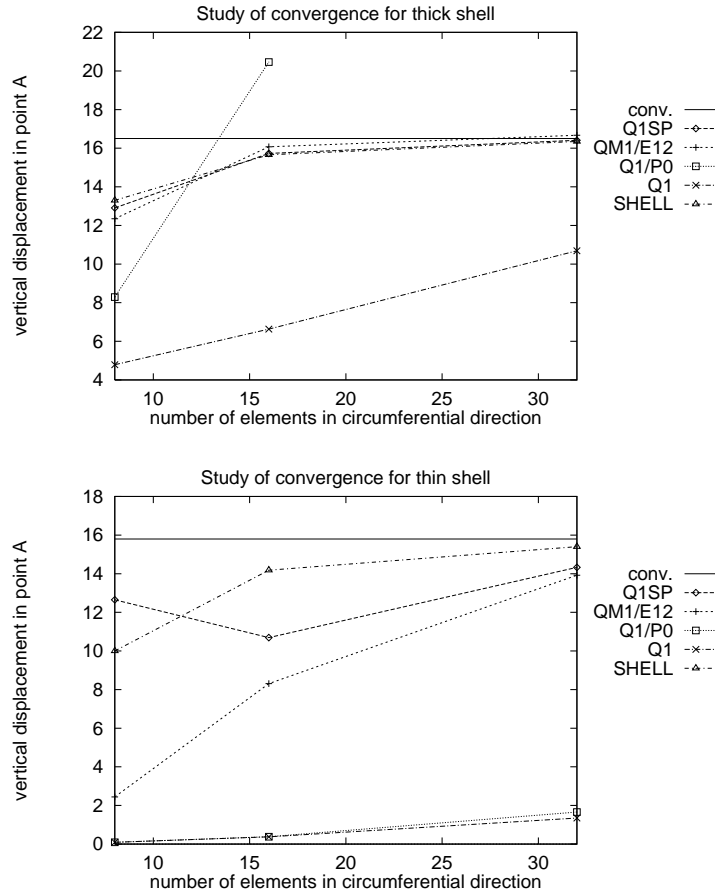


Figure 2: Cylindric shell; studies of convergence

## 4.2 Nearly incompressible block under compression

Reliable results for the present example are only provided by the B-Bar method, such that it is important to test whether the new element formulation shows a comparable performance. Geometry, loading and boundary conditions of the system are described in Figure 3. Again, only one quarter of the system is discretized, i. e. symmetry conditions have to be considered on the planes  $X_1 = 0$  and  $X_2 = 0$ . The nodes on the top of the structure are constraint in  $X_1$ - and  $X_2$ -direction. The surface load  $p_0$  is applied in the grey area on the top of the block. The material model is again a compressible Neo-Hooke model with the

material parameters  $\mu = 80.194 \text{ N/mm}^2$  and  $\Lambda = 400889.806 \text{ N/mm}^2$ .

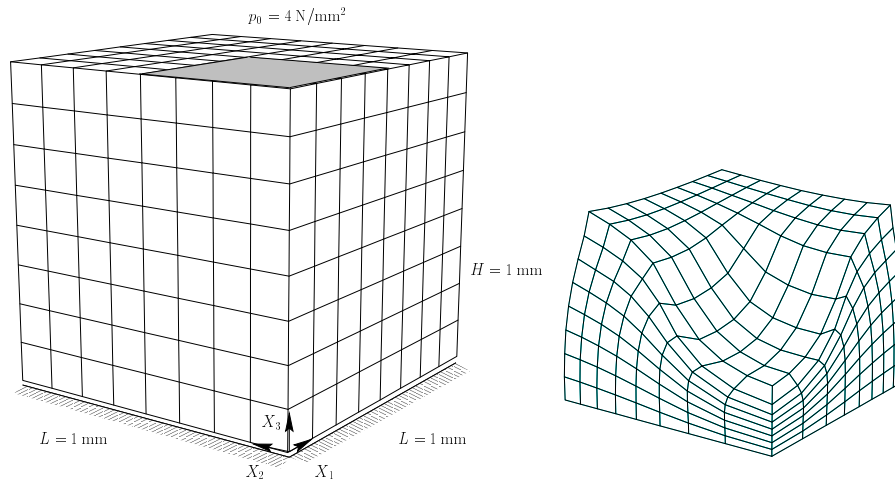


Figure 3: Block under compression

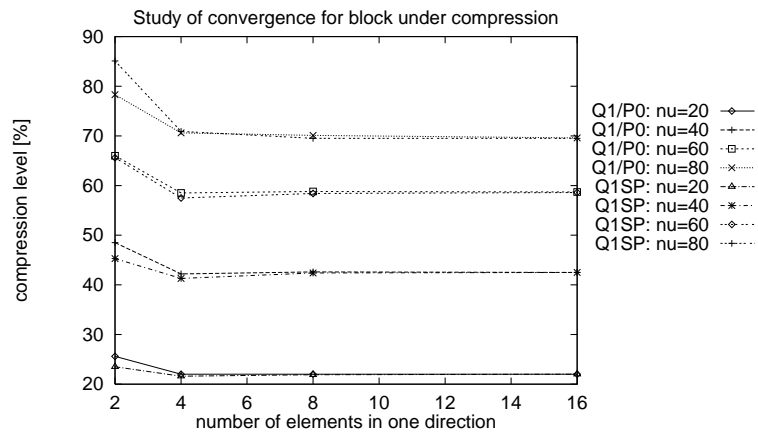


Figure 4: Block under compression; study of convergence

The convergence with increasing number of elements to the correct solution has been studied for various load levels  $\nu = p/p_0$  ( $p_0 = 4 \text{ N/mm}^2$ , Figure 4). The comparison between Q1/P0 and Q1SP shows that apart from the discretization  $2 \times 2 \times 2$ , hardly any difference in the results is noticeable. In order to ensure stability, the computation of the stabilization factors is based only on the material tangent. The standard displacement formulation Q1 shows extreme locking in this example. As expected further, the performance of QM1/E12 is here not acceptable. Numerical instabilities arise for the discretization  $4 \times 4 \times 4$  at the load level  $\nu = 39$ . The effect cannot be avoided by choosing smaller load increments which supports the hypothesis made in Section 3.2.1.

## 5 Conclusions

The examples have shown that the new element exhibits an excellent performance in bending-dominated as well as in incompressible problems. Above that, the formulation is easy to code and very efficient from the computational point of view. Numerical instabilities are avoided, if the stabilization matrix remains always positive definite. In compression, this is achieved by basing the computation of the stabilization factors rather on the material tangent than on the full tangent. Note that similar procedure is not possible for the enhanced strain method which causes difficulties especially in compression tests. A clear disadvantage of the present formulation represents, however, the dependence of the solution on the size of the load step, if the stabilization factors are only computed in the first step within each Newton iteration. Fortunately, this effect proves to be negligible in most applications. But for thin shell applications, the influence is relatively strong, making a special after-iteration procedure necessary.

The present work deals exclusively with non-linear elastic problems. Certainly, it is important to test the element also in the context of inelastic material models. This is particularly true, if the stability of the formulation is discussed. Note that in plasticity, the update of the stabilization factors becomes crucial, since the transition from the elastic to the plastic range is not continuous. Apart from this point, however, every arbitrary material model can be implemented without any modifications representing an important advantage of the new method.

## 6 Acknowledgement

The authors thank Robert Eberlein and Christian Leppin for useful discussions on important aspects of this work.

## 7 References

- [1] J. C. Simo, R. L. Taylor and K. S. Pister, Variational and projection methods for the volume constraint in finite deformation elasto-plasticity, *Computer Methods in Applied Mechanics and Engineering* **51**, 177–208 (1985).
- [2] J. C. Simo and F. Armero, Geometrically nonlinear enhanced-strain mixed methods and the method of incompatible modes, *International Journal for Numerical Methods in Engineering* **33**, 1413–1449 (1992).
- [3] J. C. Simo, F. Armero and R. L. Taylor, Improved versions of assumed enhanced-strain tri-linear elements for 3D finite deformation problems, *Computer Methods in Applied Mechanics and Engineering* **110**, 359–386 (1993).

- [4] P. Wriggers and S. Reese, A note on enhanced strain methods for large deformations, *Computer Methods in Applied Mechanics and Engineering* **135**, 201–209 (1996).
- [5] E. A. de Souza Neto, D. Peric, G. C. Huang and D. R. J. Owen, Remarks on the stability of enhanced strain elements in finite elasticity and elastoplasticity, in *Computational Plasticity – Fundamentals and Applications*, D. R. J. Owen, E. Onate and E. Hinton, eds., Pineridge Press, Swansea, 361–372 (1995).
- [6] M. A. Crisfield, G. F. Moita, G. Jelenic and L. P. R. Lyons, Enhanced lower-order element formulations for large strains, in *Computational Plasticity – Fundamentals and Applications*, D. R. J. Owen, E. Onate and E. Hinton, eds., Pineridge Press, Swansea, 293–320 (1995).
- [7] J. Korelc and P. Wriggers, Consistent gradient formulation for a stable enhanced strain method for large deformations, *Engineering Computations* **13**, 103–123 (1996).
- [8] S. Glaser and F. Armero, On the formulation of enhanced strain finite elements in finite deformations, *Engineering Computations* **14**, 759–791 (1998).
- [9] E. P. Kasper and R. L. Taylor, A mixed-enhanced strain method: finite deformation problems, Department of Civil and Environmental Engineering, University of California at Berkeley, Report No.: UCB/SEMM-97/09 (1997).
- [10] D. P. Flanagan and T. Belytschko, A uniform strain hexahedron and quadrilateral with orthogonal hourglass control, *International Journal for Numerical Methods in Engineering* **17**, 679–706 (1981).
- [11] T. Belytschko, J. S.-J. Ong, W. K. Liu and J. M. Kennedy, Hourglass control in linear and nonlinear problems, *Computer Methods in Applied Mechanics and Engineering* **43**, 251–276 (1984).
- [12] T. Belytschko and W. Bachrach, Efficient implementation of quadrilaterals with high coarse-mesh accuracy, *Computer Methods in Applied Mechanics and Engineering* **54**, 279–301 (1986).
- [13] D. Kosloff and G. A. Frazier, Treatment of hourglass pattern in low order finite element codes, *Internat. J. Numer. Analyt. Meths. Geomech.* **2**, 57–72 (1978).
- [14] D. Malkus and T. J. R. Hughes, Mixed finite element methods - reduced and selective integration techniques: a unification of concepts, *Computer Methods in Applied Mechanics and Engineering* **15**, 68–81 (1978).
- [15] S. Reese, M. Küssner and B. D. Reddy, A new stabilization technique for finite elements in finite elasticity, FRD/UCT Centre for Research in Computational and Applied Mechanics, University of Cape Town (South Africa), Report No. 287 (1998).
- [16] K. Arunakirinathar and B. D. Reddy, Some geometrical results and estimates for quadrilateral finite elements, *Computer Methods in Applied Mechanics and Engineering* **122**, 307–314 (1995).

- [17] K. Arunakirinathar and B. D. Reddy, Further results for enhanced strain methods with isoparametric elements, *Computer Methods in Applied Mechanics and Engineering* **127**, 127–143 (1995).
- [18] M. Küssner and B. D. Reddy, The equivalent parallelogram and its application in 2D and 3D finite element analysis, Proceedings of SACAM 98, Cape Town, South Africa (1998).
- [19] J. Korelc and P. Wriggers, An efficient 3D enhanced strain element with Taylor expansion of the shape functions, *Computational Mechanics* **19**, 30–40 (1996).
- [20] J. C. Simo and S. Rifai, A class of mixed assumed strain methods and the method of incompatible modes, *International Journal for Numerical Methods in Engineering* **29**, 1595–1638 (1990).
- [21] E. L. Wilson, R. L. Taylor, W. P. Docherty and J. Ghaboussi, Incompatible displacement models, in *Numerical and Computer Models in Structural Mechanics*, S. J. Fenves *et al.*, Academic Press, New York (1973).
- [22] P. Hansbo, A new approach to quadrature for finite elements incorporating hourglass control as a special case, submitted to *Computer Methods in Applied Mechanics and Engineering* (1998)
- [23] W. L. Hacker and H. L. Schreyer, Eigenvalue analysis of compatible and incompatible rectangular four-node quadrilateral elements, *International Journal for Numerical Methods in Engineering* **28**, 687–703 (1989).
- [24] U. Hueck and P. Wriggers, A formulation for the 4-node quadrilateral element, *International Journal for Numerical Methods in Engineering* **38**, 3007–3037 (1995).
- [25] N. Büchter, E. Ramm, D. Roehl, Three-dimensional extension of non-linear shell formulation based on the enhanced assumed strain concept, *International Journal for numerical methods in engineering* **37**, 2551–2568 (1994).
- [26] R. Eberlein and P. Wriggers, Finite element formulations of five and six parameter shell theories accounting for finite plastic strain, in *Computational Plasticity – Fundamentals and Applications*, D. R. J. Owen, E. Onate and E. Hinton, eds., Pineridge Press, Swansea, 1898–1903 (1997).